The dependence on the energy ratio of the shear-free interaction between isotropic turbulences

D. Tordella, M.Iovieno

Dipartimento di Ingegneria Aeronautica e Spaziale, Politecnico di Torino
Corso Duca degli Abruzzi 24, 10129 Torino, I

– D.Tordella, M.Iovieno 2005 "Numerical experiments on the intermediate asymptotics of shear-free turbulent diffusion", *Journal of Fluid Mechanics*, to appear.

– D.Tordella, M.Iovieno "The dependance on the energy ratio of the shear-free interaction between two isotropic turbulence" *Direct and Large Eddy Simulation 6 - ERCOFTAC Workshop*, Poitiers, Sept 12-14, 2005.

– D.Tordella, M.Iovieno "Self-similarity of the turbulence mixing with a constant in time macroscale gradient" *22nd IFIP TC 7 Conference on System Modeling and Optimization*, Torino, July 18-22, 2005.

– M.Iovieno, D.Tordella 2002 "The angular momentum for a finite element of a fluid: A new representation and application to turbulent modeling", *Physics of Fluids*, **14**(8), 2673–2682.

– M.Iovieno, C.Cavazzoni, D.Tordella 2001 "A new technique for a parallel dealiased pseudospectral Navier-Stokes code." *Computer Physics Communications*, **141**, 365–374.

– M.Iovieno, D.Tordella 1999 "Shearless turbulence mixings by means of the angular momentum large eddy model", *American Physical Society - 52th DFD Annual Meeting.*

Shearless turbulence mixing.

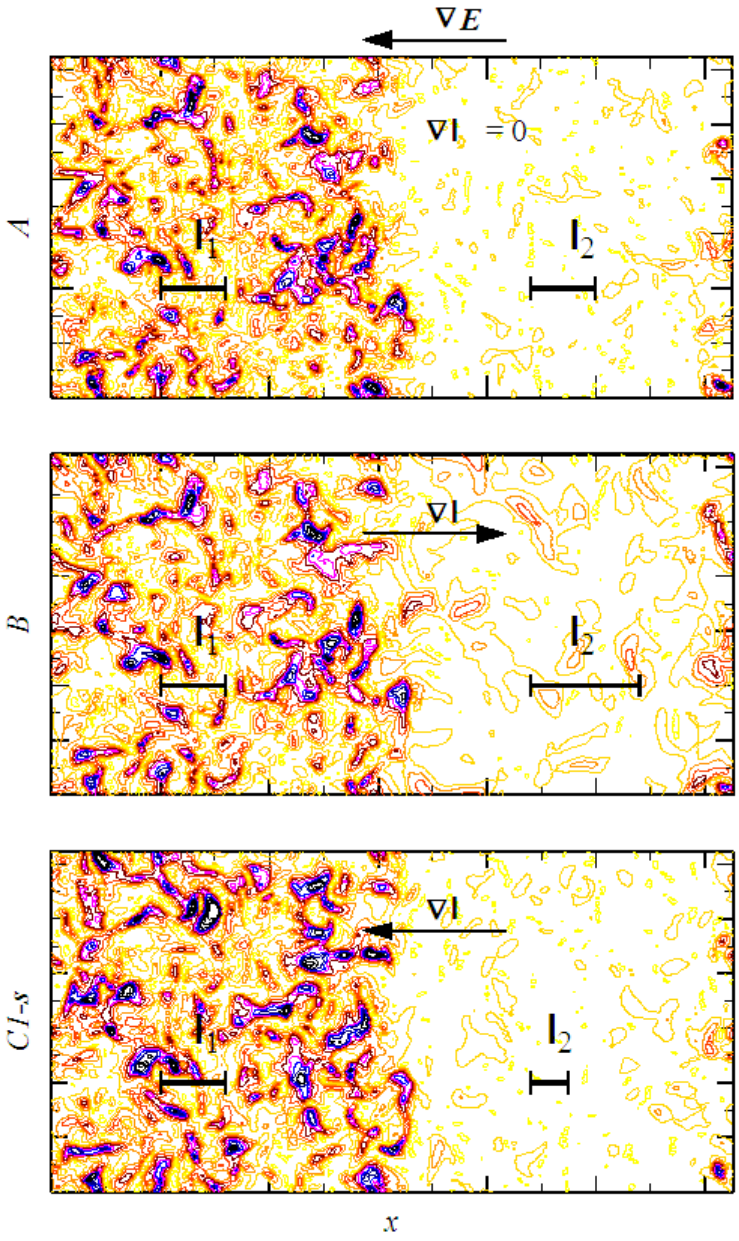

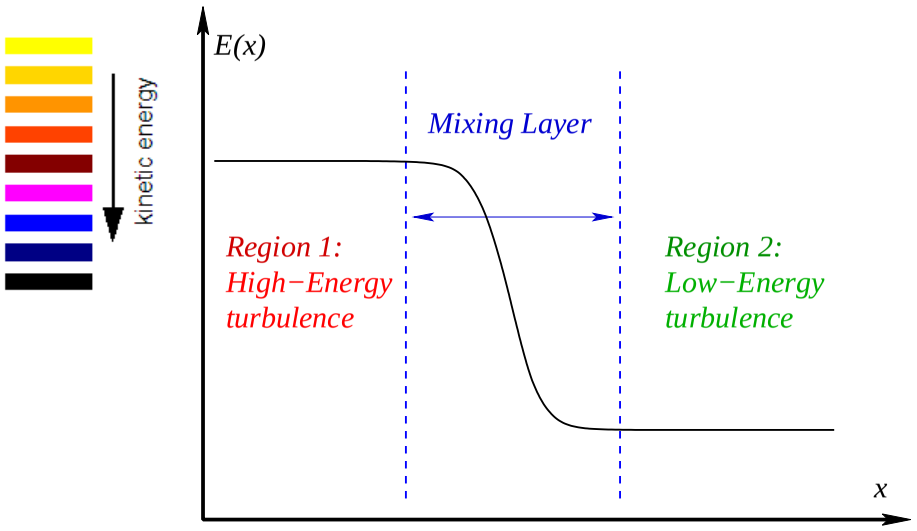

- no mean shear $\Rightarrow$ *no turbulence production*
- the mixing layer is generated by the turbulence

inhomogeneity, i.e.:

◇ by the gradient of *turbulent energy*

and

◇ by the gradient of *integral scale*

Previous investigations:

Esperiments with grid turbulence:

– Gilbert B. *J. Fluid Mech.* **100**, 349–365 (1980).

– Veeravalli S., Warhaft Z. *J. Fluid Mech.* **207**,191–229 (1989).

Numerical simulations (DNS):

– Briggs D.A., Ferziger J.H., Koseff J.R., Monismith S.G. *J. Fluid Mech.* **310**, 215–241 (1996).

– Knaepen B., Debliquy O., Carati D. *J. Fluid Mech.* **414**, 153–172 (2004).

- in (passive) grid turbulence the higher energy is always associated to larger integral scales, so the two parameters are not independent $\Rightarrow$ *guess about no intermittency in the absence of scale gradient and turbulence production*.
- numerical simulations reproduced the 3,3:1 laboratory experiment by Veeravalli and Warhaft.

New decay properties

- the two parameters, the *turbulent kinetic energy* ratio $\mathcal{E}$ and the *integral scale* ratio $\mathcal{L}$, has been independently varied
- the persistency of intermittency in the limit of no scale gradient ($\mathcal{L} \rightarrow 1$) and absence of turbulence production has been investigated.

In particular we present:

- *Part 1:* results from numerical simulations (DNS and LES, 2005 JFM, to appear)
- *Part 2:* intermediate asymptotics analysis ($\mathcal{L} \rightarrow 1$, 2005 IFIP TC7 and DLES6; $\mathcal{L} \neq 1$, in preparation)

Part 1: numerical experiments

Numerical simulations (DNS and LES) have been carried out with

- Fixed energy ratio $\mathcal{E} \sim 6.7$ and varying scale ratio $0.38 \leq \mathcal{L} \leq 2.7$
- No scale gradient ($\mathcal{L} = 1$) and variable energy ratio $1 \leq \mathcal{E} \leq 58.3$

- Reynolds number: $Re_\lambda \approx 45$ (DNS, LES) and $Re_\lambda \approx 450$ (LES, IAM model, Tordella & Iovieno *Phys.Fluids* 2002)

- Numerical method: Fourier-Galerkin pseudospectral on a $2\pi \times 2\pi \times 4\pi$ parallelepiped (Iovieno et al. *Comp.Phys.Comm.* 2001)
  Resolution: DNS $= 128^2 \times 256$, LES $= 32^2 \times 64$
- Initial conditions: two turbulent fields coming from simulations of decaying homogeneous isotropic turbulence.

Decay exponents

- The two homogeneous fields decay algebrically in time, according to theoretical (and experimental) results (see Karman and Howarth 1938, Sedov 1944, Batchelor 1953, Speziale 1995)

$$E = A(t + t_0)^{-n}$$

- Decay rates n_1, n_2 are higher than the limit, $n = 1$, for high Reynolds number, but still close to this value ($n_1 \approx n_2 \approx 1.2 - 1.4$), so that the energy and scale ratios remain nearly constant (up to 10%) during the decay

$$\frac{\mathcal{L}(t)}{\mathcal{L}(0)} = \left(1 + \frac{t}{t_{01}}\right)^{1 - \frac{n_1}{2}} \left(1 + \frac{t}{t_{02}}\right)^{-1 + \frac{n_2}{2}}$$

$$\frac{\mathcal{E}(t)}{\mathcal{E}(0)} = \left(1 + \frac{t}{t_{02}}\right)^{n_2} \left(1 + \frac{t}{t_{01}}\right)^{-n_1}$$

- All mixings have an intermediate self-similar stage of decay

Energy similarity profiles

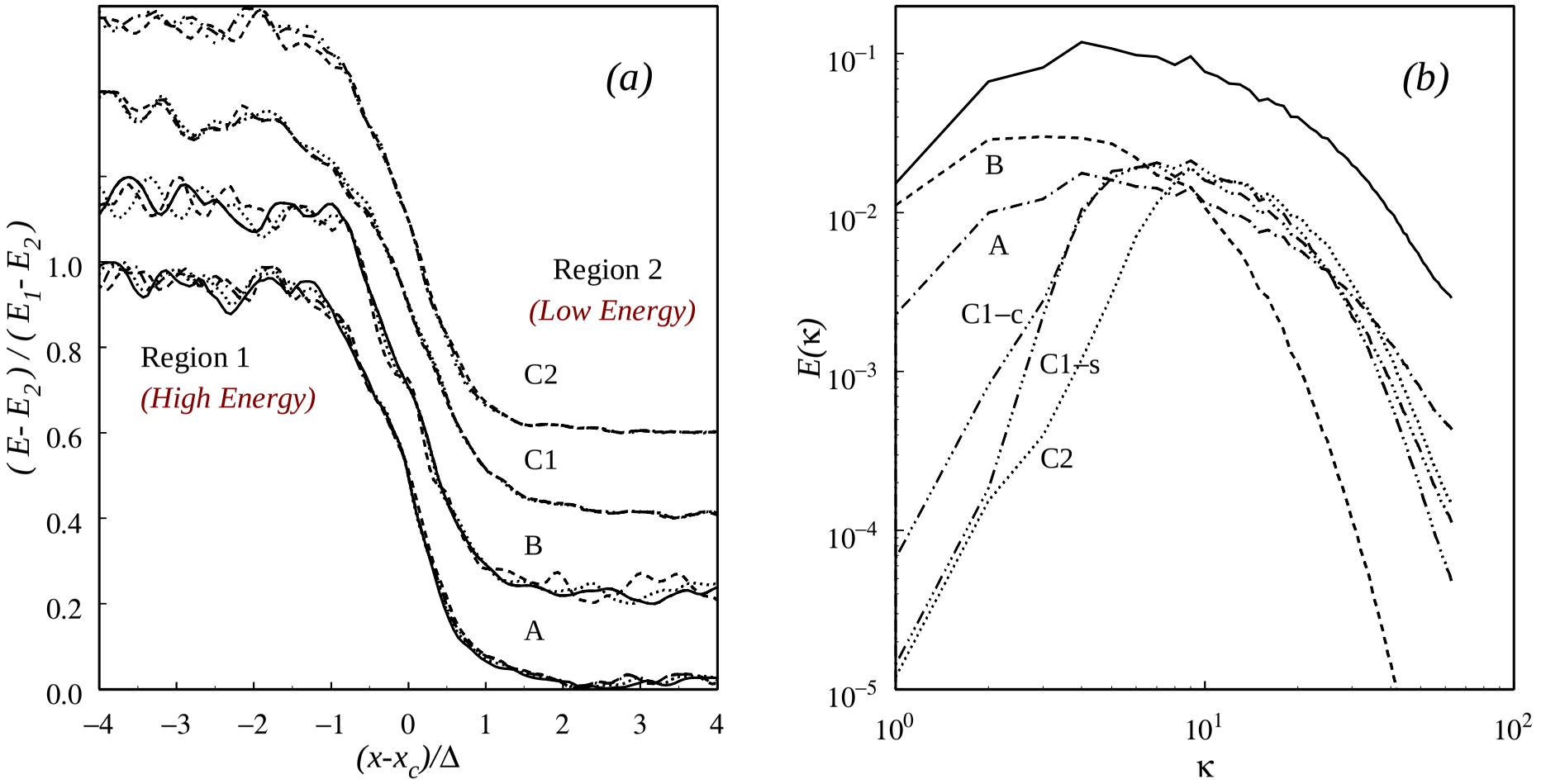

$\Delta(t)$ = mixing layer thickness, $\ell(t) = \frac{1}{3}\,\Sigma_i \frac{\int_0^\infty R_{ii}(r,t)dr}{R_{ii}(0,t)}$, where R_{ii} is the longitudinal velocity correlation (see e.g. Batchelor, 1953).

Higher order moments: skewness and kurtosis profiles

$$S = \frac{\overline{u^3}}{\overline{u^2}^{\frac{3}{2}}} \quad K = \frac{\overline{u^4}}{\overline{u^2}^2} \quad \Rightarrow \quad S \approx 0, \quad K \approx 3 \text{ in homogeneous isotropic turb.}$$

Case A: $\mathcal{E} = 6.7, \mathcal{L} = 1$, the two fields have the same integral scale.

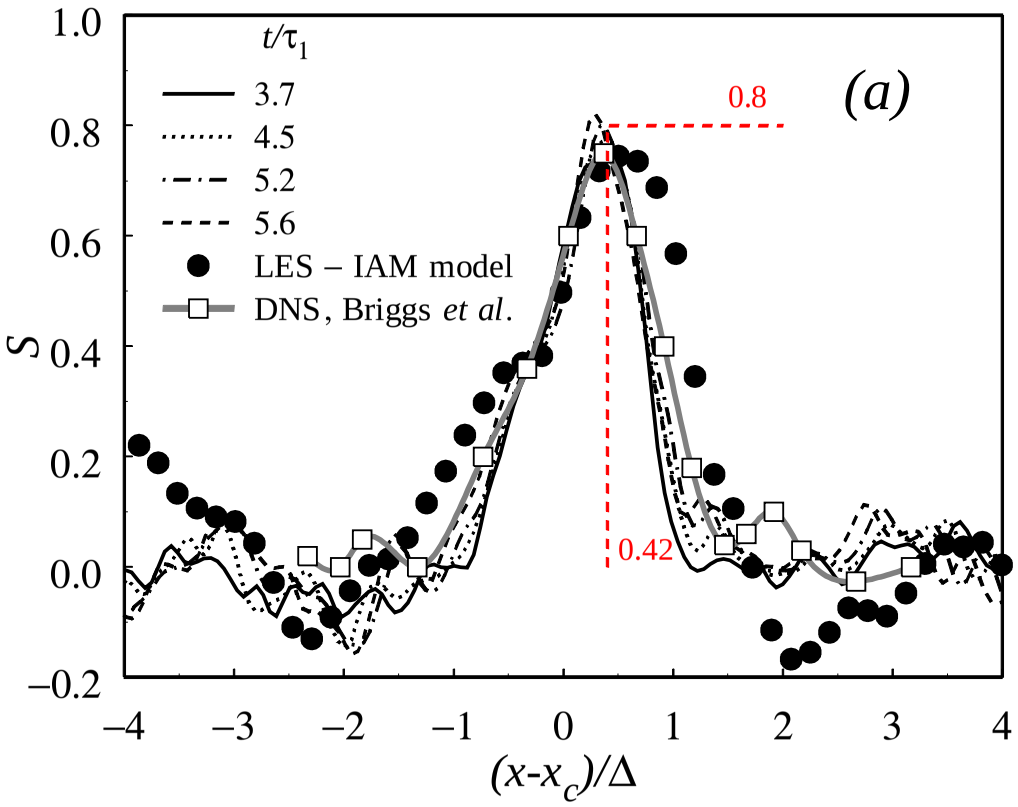

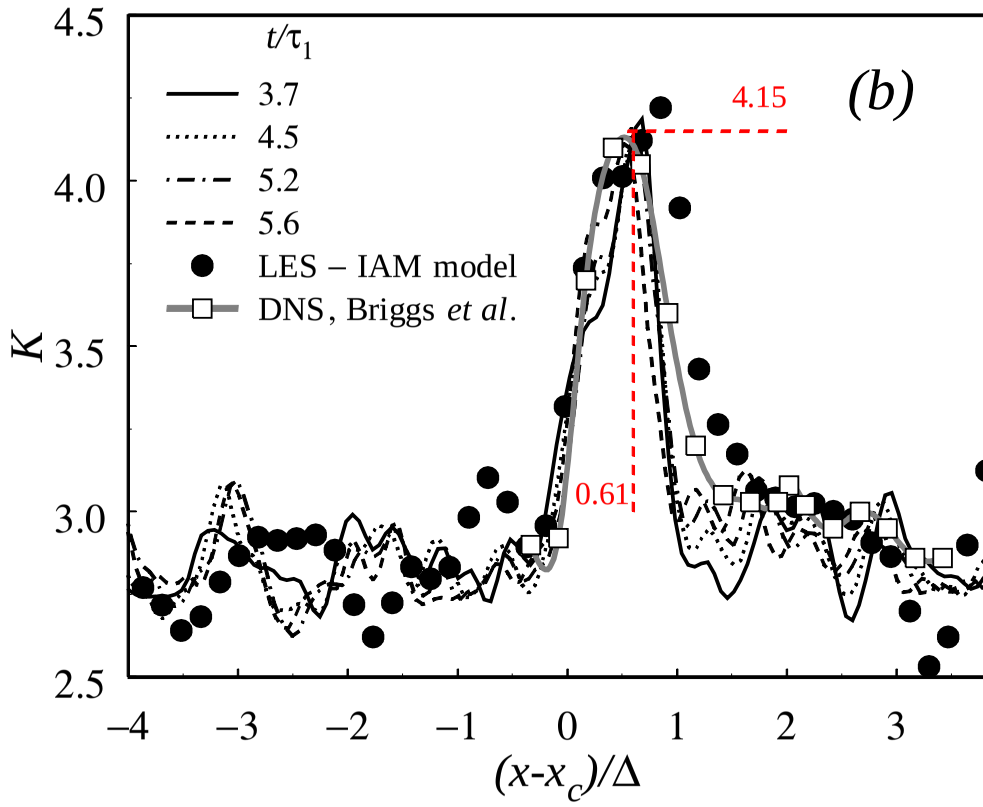

Case C: $\mathcal{E} = 6.5,\ \mathcal{L} = 1.5$: the gradients of energy and scales have the same sign: larger scale turbulence has more energy

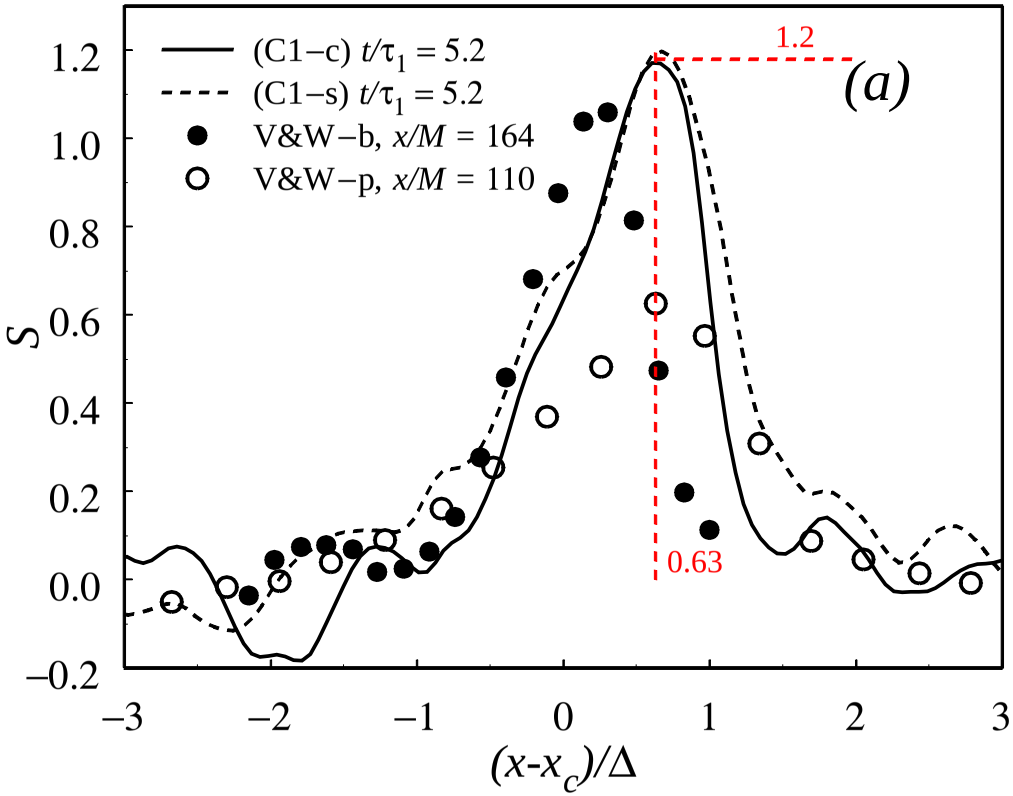

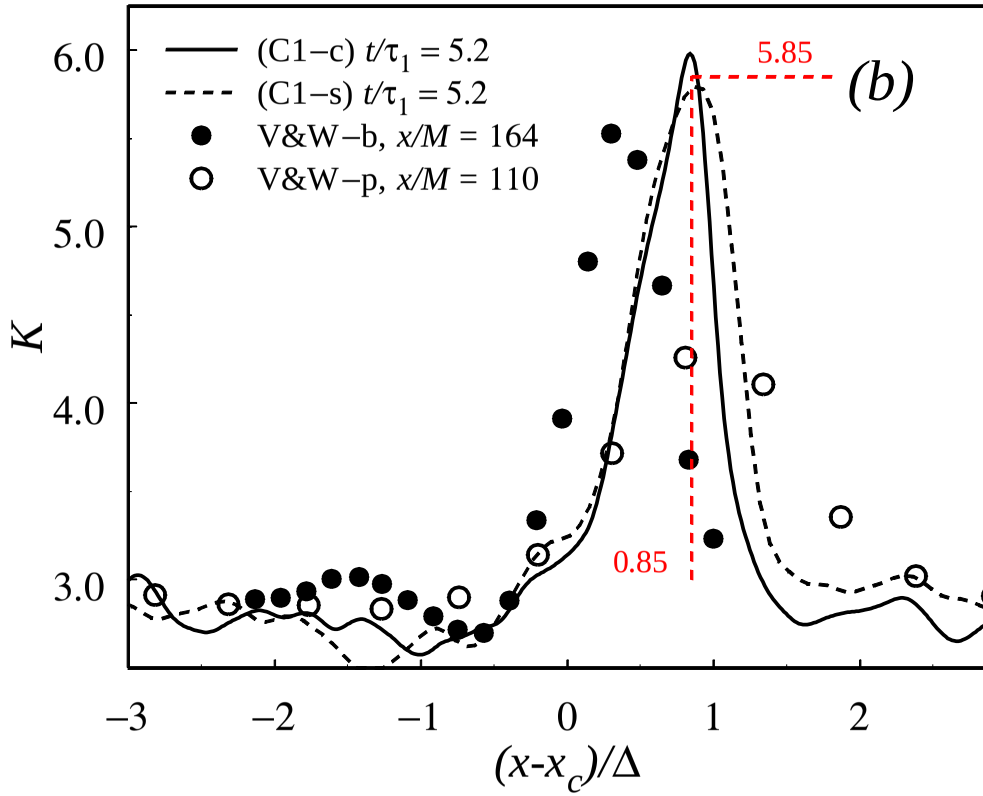

Penetration - position of the maximum of skewness/kurtosis

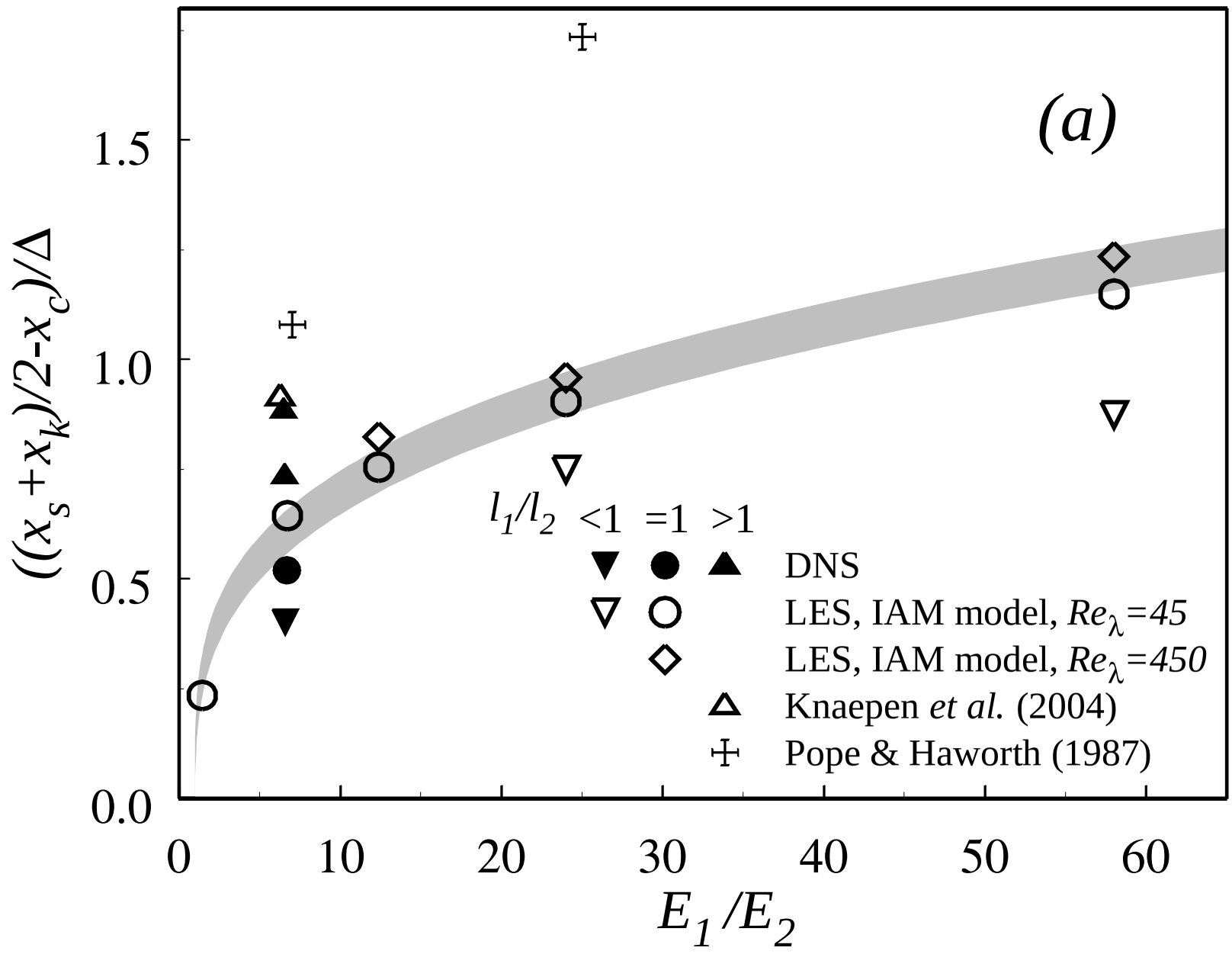

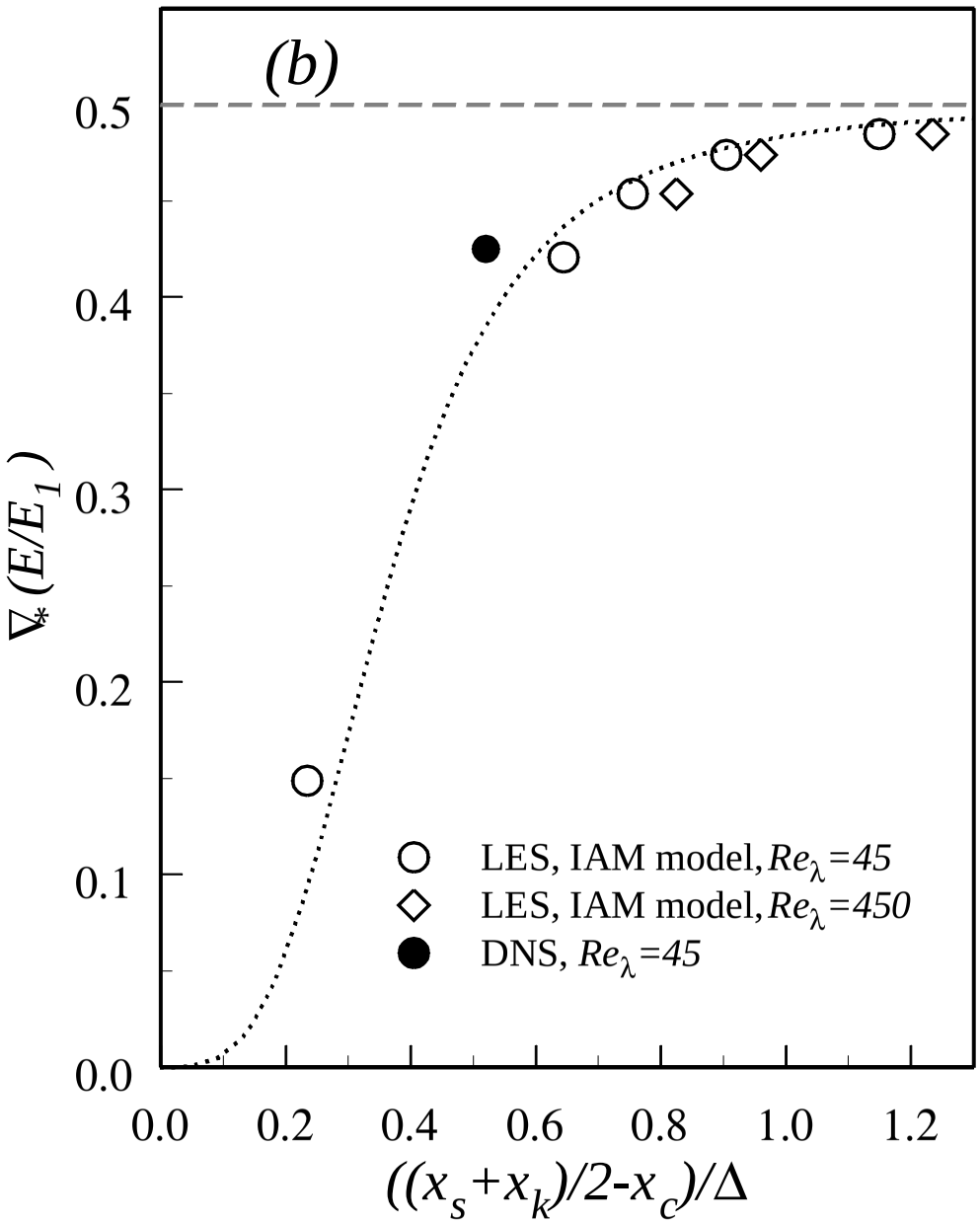

Penetration with $\mathcal{L} = 1$

Scaling law (energy ratio):

$$\frac{\eta_s + \eta_k}{2} \sim a \left(\frac{E_1}{E_2} - 1 \right)^b$$

$$a \simeq 0.36, \quad b \simeq 0.298$$

Scaling law (energy gradient):

$$\nabla_*(E/E_1) \simeq (1 - \mathcal{E}^{-1})/2$$

$$\frac{\eta_s + \eta_k}{2} \sim a \left(\frac{2\nabla_*(E/E_1)}{1 - 2\nabla_*(E/E_1)} \right)^b$$

Penetration - position of maximum of skewness/kurtosis, $\mathcal{E} = 6.7$

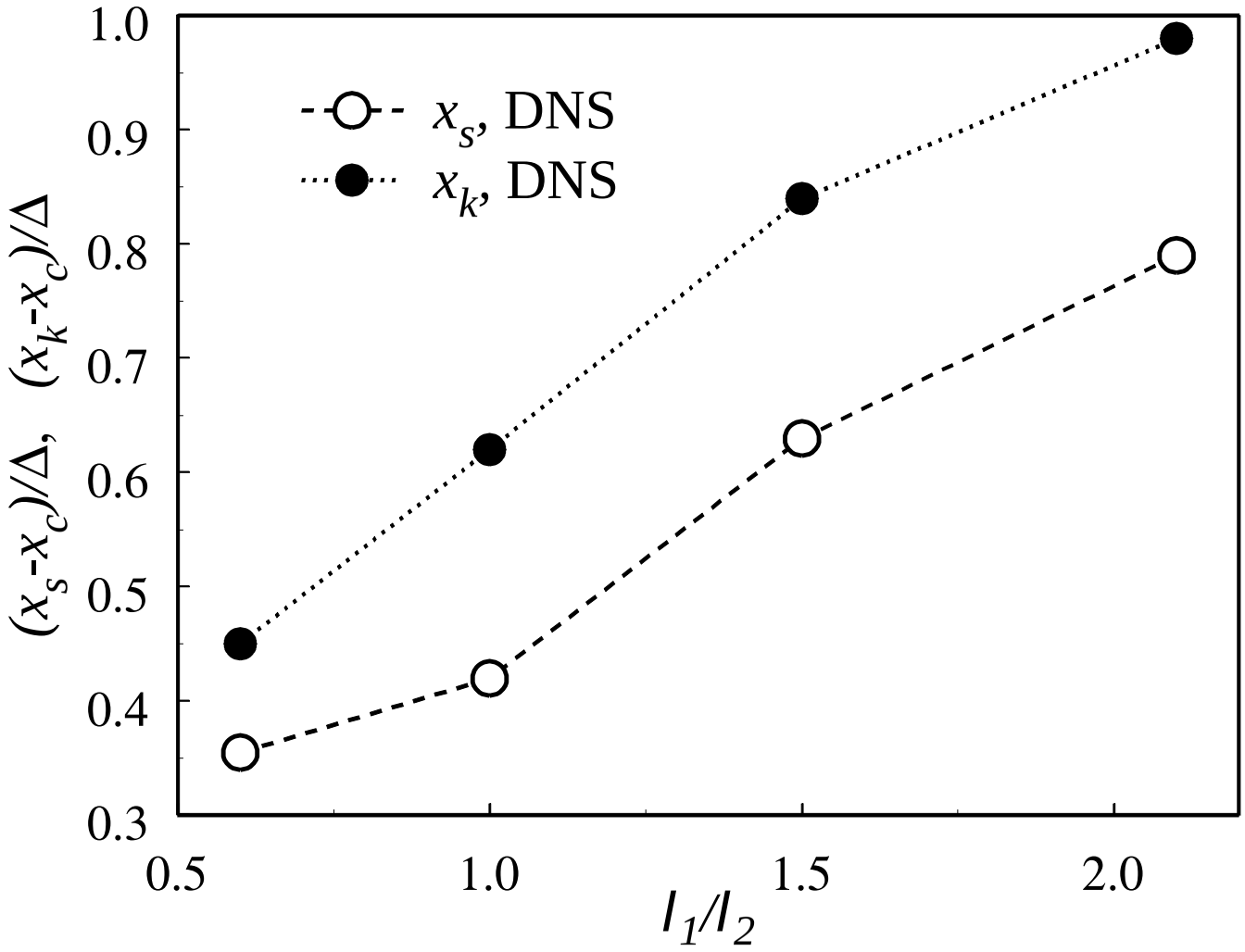

<u>Part 2:</u> similarity analysis

Properties of the numerical solutions:

- A self-similar decay is always reached
- It is characterized by a strong intermittent penetration, which depends on the two mixing parameters:
  - the turbulent energy gradient
  - the integral scale gradient

This behaviour must be contained in the turbulent motion equations:

- the two-point correlation equation which allows to consider both the macroscale and energy gradient parameters
  ($B_{ij}(\mathbf{x}, \mathbf{r}, t) = \overline{u_i(\mathbf{x}, t) u_j(\mathbf{x} + \mathbf{r}, t)}$);
- the one-point correlation equation, the limit $\mathbf{r} \rightarrow \mathbf{0}$, which allows to consider the effect of the energy gradient only.

Single-point second order correlation equations

To carry out the similarity analysis for $\mathcal{L} = 1$, we consider the second order moment equations for single-point velocity correlations

$$\partial_t \overline{u^2} + \partial_x \overline{u^3} = -2\rho^{-1}\partial_x \overline{pu} + 2\rho^{-1}\overline{p\partial_x u} - 2\varepsilon_u + \nu\partial_x^2 \overline{u^2} \quad (1)$$

$$\partial_t \overline{v_1^2} + \partial_x \overline{v_1^2 u} = 2\rho^{-1}\overline{p\partial_{y_1} v_1} - 2\varepsilon_{v_1} + \nu\partial_x^2 \overline{v_1^2} \quad (2)$$

$$\partial_t \overline{v_2^2} + \partial_x \overline{v_2^2 u} = 2\rho^{-1}\overline{p\partial_{y_2} v_2} - 2\varepsilon_{v_2} + \nu\partial_x^2 \overline{v_2^2} \quad (3)$$

where:
u is the velocity fluctuation in the inhomogeneous direction x,
v_1, v_2 are the velocity fluctuations in the plane (y_1, y_2) normal to x,
ε is the dissipation.

boundary conditions:

outside the mixing, turbulence is homogeneous and isotropic:

- For $x \to -\infty$ (high-energy turbulence):

$$\overline{u^2} = \overline{v_1^2} = \overline{v_2^2} = \frac{2}{3}E_1(t)$$

$$\overline{pu} = \overline{u^3} = \overline{v_1^2 u} = \overline{v_2^2 u} = 0$$

- For $x \to +\infty$ (low-energy turbulence):

$$\overline{u^2} = \overline{v_1^2} = \overline{v_2^2} = \frac{2}{3}E_2(t)$$

$$\overline{pu} = \overline{u^3} = \overline{v_1^2 u} = \overline{v_2^2 u} = 0$$

initial conditions:

$$\overline{u^2} = \overline{v_1^2} = \overline{v_2^2} = \begin{cases} \frac{2}{3}E_1(0) & \text{if} \quad x < 0 \\ \frac{2}{3}E_2(0) & \text{if} \quad x \geq 0 \end{cases} \qquad \overline{pu} = 0$$

Hypothesis and semplifications

- The two homogenous turbulences decay in the same way, thus

$$E_1(t) = A_1(t + t_0)^{-n_1}, \quad E_2(t) = A_2(t + t_0)^{-n_2}$$

  the exponents n_1, n_2 are close each other (numerical experiments, Tordella & Iovieno, 2005). Here, we suppose $n_1 = n_2 = n = 1$, a value which corresponds to $R_\lambda \gg 1$ (Batchelor & Townsend, 1948).

- In the absence of energy production, the pressure-velocity correlation has been shown to be approximately proportional to the convective fluctuation transport (Yoshizawa, 1982, 2002)

$$-\rho^{-1}\overline{pu} = a\,\frac{\overline{u^3} + 2\overline{v_1^2 u}}{2}, \quad a \approx 0.10,$$

- Single-point second order moments are almost isotropic through the mixing:

$$\overline{u^2} \simeq \overline{v_i^2}$$

These semplifications imply that the pressure-velocity correlations can be represented as:

$$-\rho^{-1}\overline{pu} = \alpha\overline{u^3}, \quad \alpha = \frac{3a}{1+2a} \approx 0.25.$$

Thus the problem is reduced to

$$\partial_t\overline{u^2} + (1-2\alpha)\partial_x\overline{u^3} = -2\varepsilon_u + \nu\partial_x^2\overline{u^2}$$

with the boundary and initial conditions previously described.

Similarity hypothesis

The moment distributions are determined by

- the coordinates x, t
- the energies $E_1(t)$, $E_2(t)$
- the scales $\ell_1(t)$, $\ell_2(t)$.

Thus, through dimensional analysis,

$$\begin{aligned}
\overline{u^2} &= E_1 \varphi_{uu}(\eta, R_{\ell_1}, \vartheta_1, \mathcal{E}, \mathcal{L}) \\
\overline{u^3} &= E_1^{\frac{3}{2}} \varphi_{uuu}(\eta, R_{\ell_1}, \vartheta_1, \mathcal{E}, \mathcal{L}) \\
\varepsilon_u &= E_1^{\frac{3}{2}} \ell_1^{-1} \varphi_{\varepsilon_u}(\eta, R_{\ell_1}, \vartheta_1, \mathcal{E}, \mathcal{L}),
\end{aligned}$$

where:

$\eta = x/\Delta(t)$, $\Delta(t)$ is the mixing layer thickness, $R_{\ell_1} = E_1^{\frac{1}{2}}(t)\ell_1(t)/\nu$,

$\vartheta_1 = tE_1^{\frac{1}{2}}(t)/\ell_1(t)$, $\mathcal{E} = E_1(t)/E_2(t)$, $\mathcal{L} = \ell_1(t)/\ell_2(t)$

The high Reynolds number algebraic decay ($n = 1$) implies:

$$\begin{aligned}
\mathcal{E} &= \text{const} = \frac{E_1(0)}{E_2(0)} \\
\mathcal{L} &= \text{const} = \frac{\ell_1(0)}{\ell_2(0)} \\
\vartheta_1 &= \text{const} = \frac{n}{f(R_{\lambda_1})} \\
R_{\ell_1} &\propto t^{1-n} = \text{const}
\end{aligned}$$

where $f(R_\lambda) = \dfrac{\varepsilon \ell}{E^{3/2}}$ is constant during decay (see Batchelor (1953), Speziale (1995), Sreenivasan (1998)).

$\Rightarrow \eta$ is the only similarity variable, $\eta = \eta(x, t)$.

$\Rightarrow$ **similarity conditions:**

By introducing the similarity relations in the equation and by imposing that all the coefficients must be independent from x, t, it is obtained

$$\Delta(t) \propto \ell_1(t)$$

$\Rightarrow$ **similarity equation:**

$$-\frac{1}{2}\eta\frac{\partial\varphi_{uu}}{\partial\eta} + \frac{1}{f(R_{\lambda_1})}(1-2\alpha)\frac{\partial\varphi_{uuu}}{\partial\eta} + \frac{\nu}{A_1 f(R_{\lambda_1})^2}\frac{\partial^2\varphi_{uu}}{\partial\eta^2} = \\ = \varphi_{uu} - \frac{2}{f(R_{\lambda_1})}\varphi_{\varepsilon_u}$$

with boundary conditions

$$\lim_{\eta\to-\infty}\varphi_{uu}(\eta) = \frac{2}{3}, \quad \lim_{\eta\to+\infty}\varphi_{uu}(\eta) = \frac{2}{3}\mathcal{E}^{-1}, \quad \lim_{\eta\to\pm\infty}\varphi_{uuu}(\eta) = 0$$

$\Rightarrow$ the third-order moment, φ_{uuu}, can be represented as a function of the second order moment, which yields

$$\varphi_{uuu} = \frac{1}{(1-2\alpha)}\left[\frac{f}{2}\int_{-\infty}^{\eta}\eta\frac{\partial\varphi_{uu}}{\partial\eta}\mathrm{d}\eta + \frac{\nu}{A_1 f}\frac{\partial\varphi_{uu}}{\partial\eta}\right]$$

$$S = \frac{\varphi_{uu}^{-\frac{3}{2}}}{(1-2\alpha)}\left[\frac{f}{2}\int_{-\infty}^{\eta}\eta\frac{\partial\varphi_{uu}}{\partial\eta}\mathrm{d}\eta + \frac{\nu}{A_1 f}\frac{\partial\varphi_{uu}}{\partial\eta}\right]$$

With regard to the second-order moments, the numerical experiments suggest the fit (see also Veeravalli & Wahrhaft, *JFM 1989*)

$$\frac{3}{2}\varphi_{uu} = \frac{1+\mathcal{E}^{-1}}{2} - \frac{1-\mathcal{E}^{-1}}{2}\mathrm{erf}(\eta),$$

This allows to compute the velocity skewness by analitical integration

$$S = \frac{1-\mathcal{E}^{-1}}{\sqrt{\pi}}\mathrm{e}^{-\eta^2}\left[\frac{f}{4(1-2\alpha)}\left(1-\frac{4\nu}{A_1 f^2}\right)\right]\times \left[\frac{1+\mathcal{E}^{-1}}{2} - \frac{1-\mathcal{E}^{-1}}{2}\mathrm{erf}(\eta)\right]^{-\frac{3}{2}}$$

Normalized energy and skewness distributions; $\mathcal{E} = 6.7$ and $\mathcal{L} = 1$.

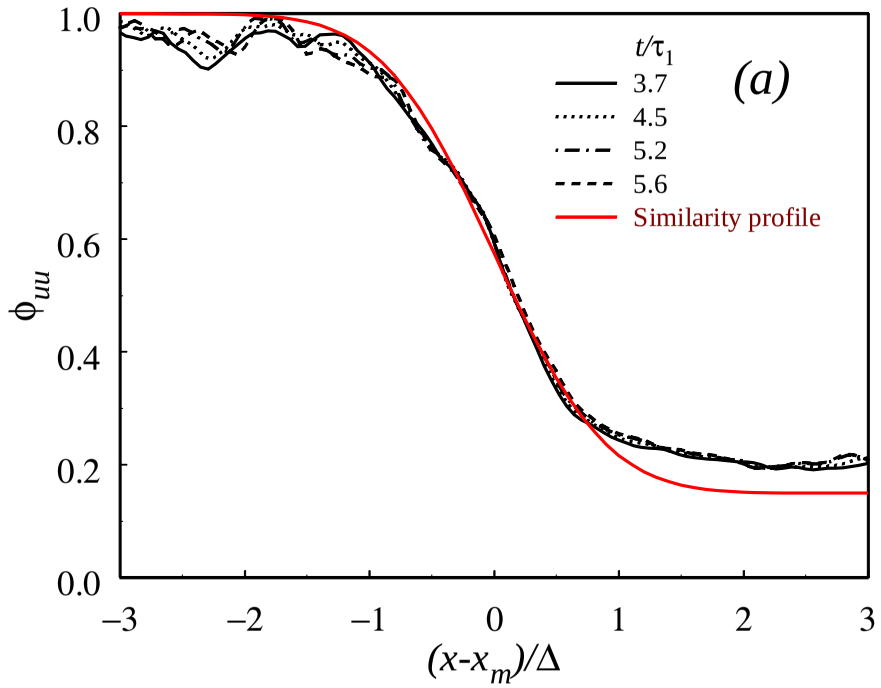

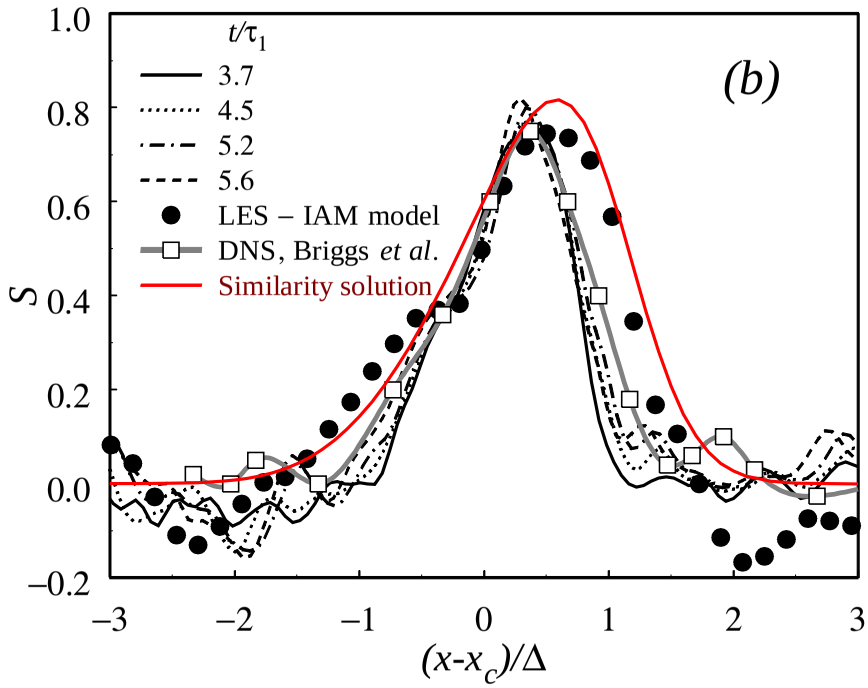

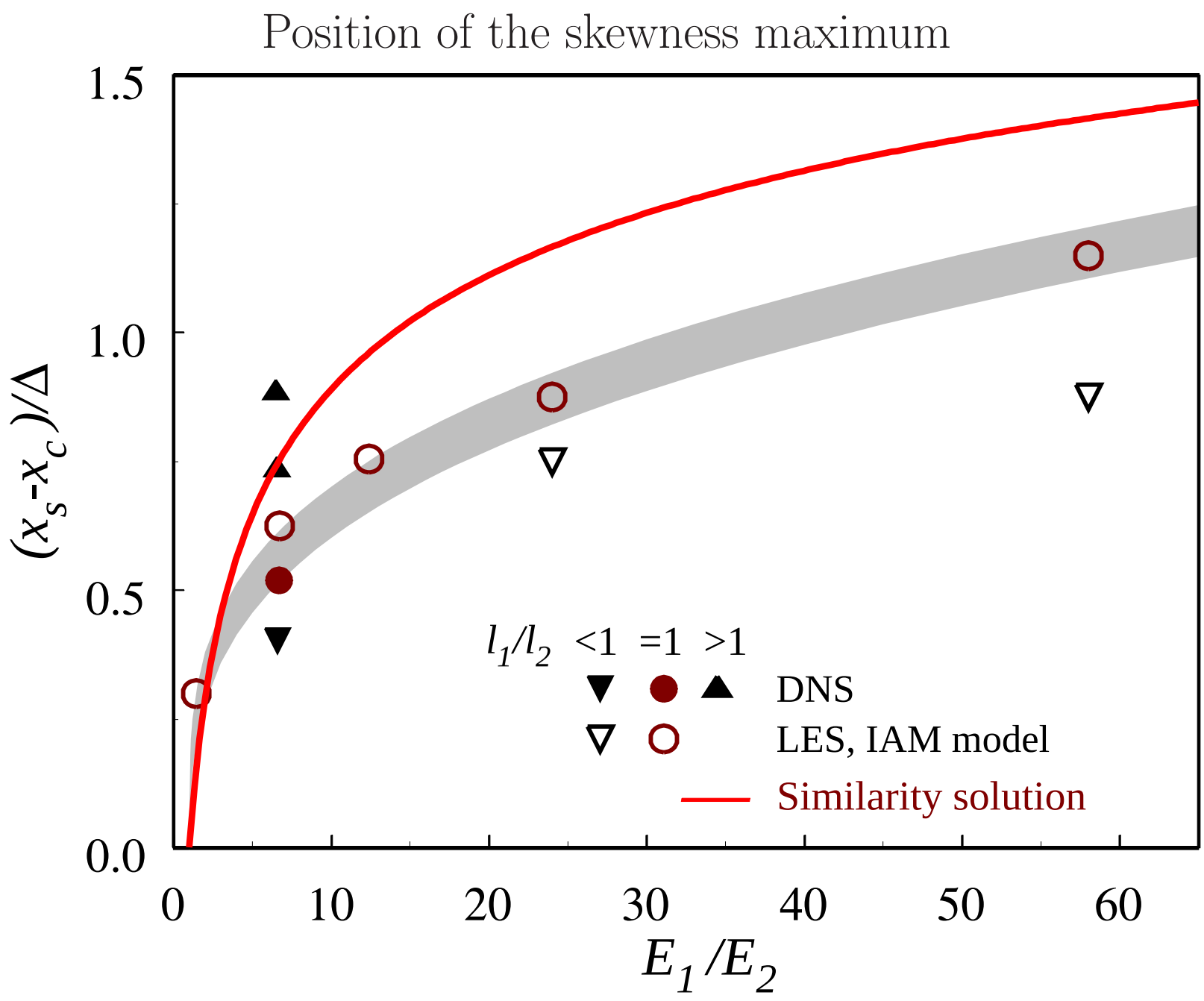
Position of the skewness maximum
1.5
1.0
0.5
0.0
$(x_s\text{-}x_c)/\Delta$
0
10
20
30
40
50
60
E_1/E_2
l_1/l_2 <1 =1 >1
DNS
LES, IAM model
Similarity solution

Conclusions

The intermediate asymptotics of the turbulence diffusion in the absence of production of turbulent kinetic energy is considered.

- An intermediate similarity stage of decay always exists.
- When the energy ratio $\mathcal{E}$ is far from unity, the mixing is very intermittent.
- when $\mathcal{L} = 1$, the intermittency increases with the energy ratio $\mathcal{E}$ with a scaling exponent that is almost equal to 0.29.
- intermittency smoothly varies when passing through $\mathcal{L} = 1$:
  it increases when $\mathcal{L} > 1$ (*concordant* gradient of energy and scale),
  it is reduced when $\mathcal{L} < 1$ (opposite gradient of energy and scale)
- the self-similar decay of the shearless mixing is consistent with the similarity solution of the single-point correlation equation.

$$
\begin{aligned}
&+ \quad \frac{\partial^2 B_{\varphi\varphi|z}}{\partial r_0^2}\frac{r_1^2 r_2^2}{r_0^4} + \frac{\partial B_{\varphi\varphi|z}}{\partial r_0}\frac{r_1^2}{r_0^3}\left(1 - 5\frac{r_2^2}{r_0^2}\right)\\
\frac{\partial^2 B_{23|3}}{\partial r_2 \partial r_3} &= \frac{\partial^2 B_{rz|z}}{\partial r_0 \partial r_z}\frac{r_2^2}{r_0^2} + \frac{\partial B_{rz|z}}{\partial r_z}\frac{r_1^2}{r_0^3}\\
\frac{\partial^2 B_{33|3}}{\partial r_1^2} &= \frac{\partial^2 B_{zz|z}}{\partial r_z^2}
\end{aligned}
$$

Sommando abbiamo:

$$
\frac{\partial^2}{\partial r_i \partial r_k} B_{ik|3} = \frac{\partial^2 B_{rr|z}}{\partial r_0^2} + \frac{2}{r_0}\left(\frac{\partial B_{rr|z}}{\partial r_0} - \frac{\partial B_{\varphi\varphi|z}}{\partial r_0}\right) + 2\frac{\partial^2 B_{rz|z}}{\partial r_0 \partial r_z} + \frac{2}{r_0}\frac{\partial B_{rz|z}}{\partial r_z} + \frac{\partial^2 B_{zz|z}}{\partial r_z^2} \tag{117}
$$

Inoltre, dal momento che

$$
B_{31|3} = B_{rz|z}\frac{r_1}{r_0}, \quad B_{32|3} = B_{rz|z}\frac{r_2}{r_0}, \quad B_{33|3} = B_{zz|z}
$$

e quindi

$$
\begin{aligned}
\frac{\partial^2 B_{31|3}}{\partial r_1^2} &= \frac{\partial B_{rz|z}}{\partial r_0}\frac{r_1^2}{r_0^2} + B_{rz|z}\frac{r_2^2}{r_0^3}\\
\frac{\partial^2 B_{32|3}}{\partial r_2^2} &= \frac{\partial B_{rz|z}}{\partial r_0}\frac{r_2^2}{r_0^2} + B_{rz|z}\frac{r_1^2}{r_0^3}\\
\frac{\partial^2 B_{33|3}}{\partial r_3^2} &= \frac{\partial B_{zz|z}}{\partial r_z}
\end{aligned}
$$

per cui:

$$
\frac{\partial^2 B_{3k|3}}{\partial x_3 \partial r_k} = \frac{\partial^2 B_{rz|z}}{\partial z \partial r_z} + \frac{1}{r_0}\frac{\partial B_{rz|z}}{\partial z} + \frac{\partial^2 B_{zz|z}}{\partial z \partial r_z}
$$

In conclusione, l'equazione è:

$$
\begin{aligned}
\left(-\frac{\partial^2}{\partial z^2} + 2\frac{\partial^2}{\partial z \partial r_z} + \frac{\partial^2}{\partial r_0^2} + \frac{1}{r_0}\frac{\partial}{\partial r_0} + \frac{\partial^2}{\partial r_z^2}\right) B_{pz} &= \left(\frac{\partial^2}{\partial z^2} - 2\frac{\partial^2}{\partial z \partial r_z} + \frac{\partial^2}{\partial r_z^2}\right) B_{zz|z}\\
-2\left(\frac{\partial^2}{\partial z \partial r_0} + \frac{1}{r_0}\frac{\partial}{\partial z} - \frac{1}{r_0}\frac{\partial}{\partial r_0}\right) B_{rz|z} &+ \left(\frac{\partial^2}{\partial r_0^2} + 2\frac{\partial^2}{\partial r_0 \partial r_z} + \frac{2}{r_0}\frac{\partial}{\partial r_0}\right) B_{rz|z} +\\
&+ \frac{2}{r_0}\left(B_{rr|z} - B_{\varphi\varphi|z}\right)
\end{aligned} \tag{118}
$$

$$[f]_{(i)}=(2\delta)^{-2}\int_{-\delta}^{\delta}\int_{-\delta}^{\delta} f(\mathbf{x}+\eta_j\mathbf{e}_j+\eta_k\mathbf{e}_k)\mathrm{d}\eta_j\mathrm{d}\eta_k .$$

Nikolaevskij neglects the terms $O(\delta^2)$. In so doing, he loses the symmetry of the tensors involved in the equations, together with the commutability.

In the application of the microfluid theory to turbulence, by Eringen,[13] the turbulent flow is considered as the motion of a simple microfluid, even though any physical internal structure that could cause asymmetry is missing.

The motion of the micropolar element is described by the mean velocity $v_k(\mathbf{x},t)$ and by the microgyration tensor $\nu_{kl}(\mathbf{x},t)$ $(k,l=1,2,3)$. The latter arises from the motion and deformations of material points inside the volume of the microelement. The resulting system of equations—which are not reducible to the filtered Navier–Stokes equations—comprehends 12 scalar equations for the three components of the mean velocity and for the nine components of $\nu_{kl}(\mathbf{x},t)$ and contains 23 constant viscosity coefficients. The intrinsic moment of the momentum equation, which can be obtained from the antisymmetrical part of $\nu_{kl}(\mathbf{x},t)$, is coupled to the momentum equation through the antisymmetrical part of the stress tensor, as in Mattioli and Nikolaevsky. In his solution for the two-dimensional (2-D) turbulent channel flow, Eringen gives a solution of his system of equations where the stress tensor is nonsymmetric. The constant coefficients, which are only five thanks to the simple domain geometry, were adjusted according to the experimental observations by Laufer.[17] However, it is easily seen that if the nonsymmetric part of the stress tensor is placed equal to zero, the equations result to be uncoupled and the mean motion would be independent of the internal motion of the microelements.

B. Angular momentum large eddy model for turbulent flows

In this paragraph we would like to propose a different kind of coupling of the momentum and angular momentum equations, which does not require that a nonsymmetry part of the stress tensor exists. In the framework of the large eddy scale simulation, a new differential model is proposed for the turbulent stresses that is based on a Boussinesq transport coefficient that is proportional to the mean intrinsic moment modulus h, a flow integral quantity that takes into account velocity derivatives of any odd order [see Sec. II, Eqs. (6) and (7)], and that is supposed to include both the mechanims of stretching and the process of autodiffusion. The coupling between the momentum and moment of momentum equations is thus given by the functional dependence of the eddy diffusivity over the intrinsic angular momentum of a finite volume of a fluid. Let us consider the incompressible momentum equation,

$$\partial_t(u_k)+\partial_{\not\ell}(u_k u_{\not\ell})=\frac{1}{\rho}\partial_{\not\ell}\sigma_{k\not\ell}+b_k ,$$

where $\sigma_{k\not\ell}$, b_k are the stress tensor and the external field, respectively. Applying the average operator $\langle\cdot\rangle_\delta$, the momentum equation is written in the following form:

$$\mathrm{D}_t\langle u_i\rangle=\rho^{-1}\partial_j\langle\sigma_{ij}\rangle+\partial_j\tau_{ij}+\langle b_i\rangle, \tag{14}$$

where $\tau_{ij}=\langle u_i\rangle\langle u_j\rangle-\langle u_i u_j\rangle$ is the turbulent momentum flow per unit mass. The intrinsic angular momentum equation is obtained by applying the operator $\mathbf{M}$ [relation (2) in Sec. II] to the incompressible Navier–Stokes equation. The addition of the term $\varepsilon_{i\not\ell k}[(\langle x_l u_k\rangle-\langle x_l\rangle\langle u_k\rangle)\langle u_j\rangle]$—the convection of the intrinsic angular momentum per unit mass by means of the averaged velocity field—to each side of the resulting balance yields the following equation for h_i, that is, the intrinsic angular momentum per unit mass of the element $\mathcal{I}_\delta$ [see (7), Sec. II]:

$$\mathrm{D}_t h_i=\rho^{-1}\partial_j\varsigma_{ij}+\partial_j c_{ij}+\beta_i , \tag{15}$$

where

$$c_{ij}=\varepsilon_{i\not\ell k}[(\langle x_l u_k\rangle-\langle x_l\rangle\langle u_k\rangle)\langle u_j\rangle-(\langle x_l u_k u_j\rangle-\langle x_l\rangle\langle u_k u_j\rangle)], \tag{16}$$

$$\varsigma_{ij}=\varepsilon_{i\not\ell k}(\langle x_l\sigma_{kj}\rangle-\langle x_l\rangle\langle\sigma_{kj}\rangle), \tag{17}$$

$$\beta_i=\varepsilon_{i\not\ell k}(\langle x_l b_k\rangle-\langle x_l\rangle\langle b_k\rangle), \tag{18}$$

are, respectively, the inertial (containing stretching) and interaction flow tensors of angular momentum and $\boldsymbol{\beta}$ is the couple associated to the external field $\mathbf{b}$.

The terms inside Eqs. (14) and (15) that need to be represented through a model are the turbulent momentum and angular momentum stresses. The functional relations on which the model relies are all Galilean invariants and are listed below:

$$\nu_\delta=ch, \tag{19}$$

$$\tau_{ij}=ch(\partial_j\langle u_i\rangle+\partial_i\langle u_j\rangle-\tfrac{2}{3}\partial_k\langle u_k\rangle\delta_{ij}), \tag{20}$$

$$c_{ij}=\langle u_i\rangle h_j+ch(\partial_j h_i+\partial_i h_j-\tfrac{2}{3}\partial_k h_k\delta_{ij}), \tag{21}$$

where c is a subgrid constant.

The first term on the right-hand side of (21) represents the role played by the stretching, while the other simulates the momentum transfer due to the turbulent convection. The present day reference large eddy simulation method is based on the adoption of Smagorinsky's[18] or the vorticity[19] models, which assume a local invariance of the turbulent motion. Thus, in the immediate vicinity of a point, in time and space, a dynamical similarity is assumed throughout the field. The nondimensionalization of the field is based on the existence of local turbulent scales that are small enough to adjust to the slowly changing environment in the external scale. With this model one degree of freedom is introduced—the intrinsic angular momentum—which is portrayed by a relevant differential equation, which is coupled but, however, independent of the momentum equation. In this way we also hope to be able to simulate a turbulent flow that is not in local equilibrium. This would, of course, depend on the propriety with which the turbulent flow tensor of the intrinsic moment of momentum is modeled. In relation (21) it was attempted to insert the two major inertial phenomena that are present at the level of the subgrid scales, the stretching and the transport due to the turbulent convection.

In spite of the introduction of an additional differential equation, only one subgrid constant c appears in the model.

Assuming that the largest resolvable wave number lies within the inertial range, that the energy transferred from the resolved scales to the subgrid scales is equal to the energy dissipated by the latter and that the energy of the subgrid scales is that contained by their inertial part (see Lilly[20] and Yoshizawa[21]) constant c may be estimated as 0.066 (see Appendix A for details).

Note that in local turbulence equilibrium conditions the scaling of the turbulent viscosity, with respect to the dissipation function ϵ and the filtering length δ, is the same as that of the intrinsic angular momentum,

$$h \sim \delta^{4/3}\epsilon^{1/3} \sim \nu_\delta. \tag{22}$$

For the derivation of these scaling laws see Monin and Yaglom[22] as regards h and Yoshizawa,[21] Leslie and Quarini[23] as regards ν_δ.

As a comment on the functional structure of the present model, it is possible to draw a parallel between the latter and the mixed subgrid model (Bardina *et al.*, 1980):[24]

$$\tau_{ij}^{\mathrm{mix}} = c_{\mathrm{sim}}(\langle\langle u_i\rangle\rangle\langle\langle u_j\rangle\rangle - \langle\langle u_i\rangle\langle u_j\rangle\rangle) + 2(c_s\delta)^2|\langle D\rangle|\langle D_{ij}\rangle,$$

where c_{sim} and c_s are the similarity and Smagorinsky subgrid coefficients and D_{ij} is the strain rate tensor. The analogy consists in the fact that the first terms of the expansions in series of δ of the similarity subgrid tensor τ_{ij}^{sim} and of the real subgrid tensor ($\tau_{ij} = \langle u_i\rangle\langle u_j\rangle - \langle u_i u_j\rangle$) are both proportional to $\partial_m u_i \partial_m u_j \delta^2$, while the first terms of the expansions in series of δ of relation (21) and of the inertial tensor of the flow of intrinsic angular momentum (16) are both proportional to $u_i \omega_j \delta^2$ (see Appendix B for details). From this aspect we can infer that the present model could feature a certain degree of backscatter: directly on h_i and indirectly on ν_δ. Also of interest is the fact that—in the context of spectral numerical simulations—the number of spectral products that are necessary to implement the angular momentum model, in spite of the fact that it is a differential model, is exactly the same as the number of spectral products that are necessary to implement the mixed model.

In short, the main features of this model are the following: the capability of following the evolution of h, and thus of ν_δ, through a relevant differential equation and the proper scaling with respect to the filtering length and the dissipation rate. The differential nature would suggest an employment of nonequilibrium turbulent flows for simulations.

A unique feature of the present model is its natural convenience to simulate the dynamics of structured fluid in turbulent motion. In this case, the coupling between the momentum and angular momentum equations already having been introduced by the physics of the system, the model reduces from differential to algebraic.

C. Numerical validation of the angular momentum large eddy model

The results obtained from tests concerning the statistical and spectral properties of (i) homogeneous and isotropic turbulence, (ii) homogeneous turbulence undergoing a solid body rotation, and (iii) shear-free nonhomogeneous turbulence are presented in this section.

Before beginning the discussion on the numerical tests, the criteria adopted to carry out the comparison of the angular momentum model in the simplest way with different subgrid models are described—the Smagorinsky and the mixed models—being chosen as reference. Since an optimized value for the angular momentum model subgrid constant is not yet available at this stage, all the models are considered through their basic representation, which is founded on a subgrid scale coefficient deduced from the knowledge of only the Kolmogorov constant [Lilly's value[20] for the Smagorinsky model; see Bardina *et al.* (1980)[24] and Meneveau and Katz (1996)[25] for the mixed model and Appendix A for the present model]. In this way it has been attempted to free the analysis from the peculiarities of the optimization process, which is always based on empirical information, which, if not known well and reproduced, could spoil the mutual comparisons of the models. Our analysis is mostly carried out using the very basic values of the subgrid coefficients, with a few supplements of information relevant to the Smagorinsky and mixed models—utilized with optimized coefficients[25]—to be introduced into the comparative analysis, where opportune. On the other hand, to escape from the complexity linked to the introduction of a further step in the modeling process, we will also avoid comparing the models in the version that arises from the implementation of the dynamical procedure,[26] which, nevertheless, could always be adopted to substantially improve the performance of all the subgrid models (see the review by Meneveau and Katz, 2000).[25] The angular momentum subgrid model could, of course, undergo the dynamical procedure as could any other subgrid scale model.

The homogeneous and isotropic field used as the initial condition for all the large eddy simulations carried out to validate the present model is the 512^3 DNS database by Wray.[27] The initial distribution of the volume-averaged velocities and intrinsic moment of momenta are determined by averaging Wray's data over cubes with 2δ sides corresponding to a LES spatial resolution of 64^3 points.

The energy temporal decays of homogeneous and isotropic turbulence, obtained from pseudospectral Navier–Stokes simulations over 64^3 points, implementing the angular momentum, the Smagorinsky and the mixed models, are shown in Fig. 1(a), together with the decay produced by the direct numerical simulation by Wray[27] over 512^3 points.

To make the LES temporal decays, obtained after filtering the DNS data, and the DNS decay comparable, the last decay is also shown after having applied at each instant a low-pass filter on the spectral energy that consists of the integration of the three-dimensional energy spectrum—included in the database at different eddy turnover times—over the lowest 32 wave numbers, which is equivalent to a spatial resolution of 64^3 points for the large eddy simulations.

The angular momentum model behaves well, since it performs slightly better than the basic Smagorinsky and the mixed models. The performances become equivalent if the